Communication

Time-Resolved Electrochemical Detection of Discrete Adsorption Events

Bernadette M. Quinn, Pieter G. van 't Ho, and Serge G. Lemay

J. Am. Chem. Soc., **2004**, 126 (27), 8360-8361• DOI: 10.1021/ja0478577 • Publication Date (Web): 17 June 2004

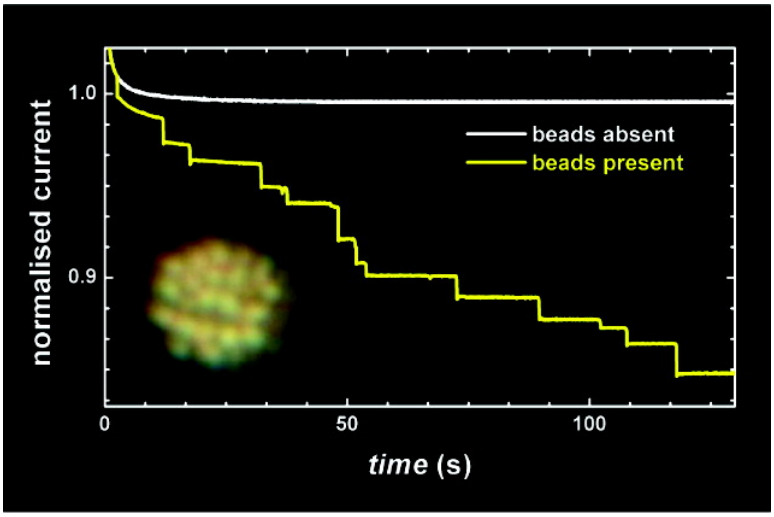

More About This Article

Additional resources and features associated with this article are available within the HTML version:

- Supporting Information
- Access to high resolution figures
- Links to articles and content related to this article
- Copyright permission to reproduce figures and/or text from this article

View the Full Text HTML

J|A|C|S
COMMUNICATIONS

Published on Web 06/17/2004

Time-Resolved Electrochemical Detection of Discrete Adsorption Events

Bernadette M. Quinn, Pieter G. van 't Hof, and Serge G. Lemay*

Kavli Institute of Nanoscience, Delft University of Technology, Lorentzweg 1, 2628 CJ Delft, The Netherlands

Received April 14, 2004; E-mail: lemay@mb.tn.tudelft.nl

This communication reports the amperometric detection of single carboxylated micro- and nanospheres adsorbing on electrodes as well-resolved, discrete steps in the current−time response. Detection at the single-event level is a necessary requirement for a range of single-molecule experiments and can greatly enhance existing sensor technologies.[1] Electrochemical detection of micron-sized latex beads at arrays of microelectrodes has also been proposed as a sensing technique for use in sandwich-type immunoassays, and it was deduced that single-bead detection could be realized.[2] Here it is demonstrated that the binding of individual beads to an electrode of comparable size can be unequivocally determined. Furthermore, we show that the principle can be successfully scaled down to detect 50 nm spheres at 100 nm-sized electrodes. Calculations suggest that the detection of single-protein binding events will be feasible with the advent of stable nanometer electrodes.

The amperometric detection method described here consists of electrolyzing a solution redox mediator, ferrocene methanol (FcMeOH), at an Au microdisk electrode (BAS, radius $r_e = 2.5$ μm) and recording the corresponding current−time transients in the absence and presence of microspheres (carboxylated latex beads, IDC, Oregon, $r_b = 0.5$ and 0.15 μm).[3] Examples of typical current−time ($I-t$) transients obtained are given in Figure 1a,b.

The beads are not electroactive, and the steplike decreases in current ΔI apparent in Figure 1 correspond to the blocking of FcMeOH mass transfer by individual beads approaching the electrode surface. It can be clearly seen that the average time interval between events, Δt, is strongly dependent on the salt concentration added to solution: the number of steps in Figure 1 increases from one at 50 mM KCl to ca. 30 and 100 for 5 and 0.5 mM, respectively. This electrophoretic rate of beads arriving at the electrode,[2] J_{mig}, is a consequence of the electric field in bulk solution due to the oxidation current at the electrode and is given to a good approximation by the simple expression

$$J_{mig} = \frac{1}{\Delta t} \approx \frac{I c_{bead}}{e c_{KCl}} \left(\frac{u_{bead}}{u_{K^+} + u_{Cl^-}} \right) \qquad (1)$$

Here, I is the anodic current response at the disk electrode, e is the unit of charge, and c and u refer to concentrations and mobilities, respectively (Supporting Information). J_{mig} is estimated as 0.50, 0.06, and 0.003 s^{-1} for 0.5, 5, and 50 mM KCl,[5] comparable with the rates of 0.43, 0.1, and 0.005 s^{-1} observed in Figure 1 up to monolayer coverage. Systematic variation of the bead and salt concentrations (c_{bead} and c_{KCl}) and current (I) demonstrated that the bead flux is proportional to I and c_{bead} and inversely proportional to c_{KCl}. In Figure 2, the linear dependence of values determined for $1/\Delta t$ from each measurement vs the grouped variable $c_{bead}I/c_{KCl}$ confirms the validity of eq 1 to describe bead arrival rate. We attribute the slight deviation in the low-rate regime to the dependence of bead mobility u_{bead} on the salt concentration.[5b,c] Beads can also approach the surface by diffusion, but the corresponding rate[4] is insignificant compared to that due to migration

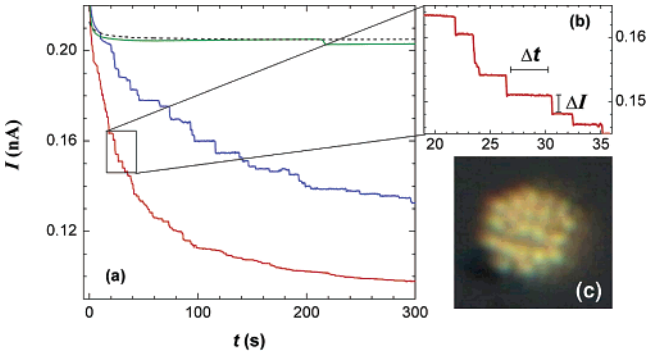

Figure 1. (a) Current−time ($I-t$) transients for the diffusion-limited oxidation of 0.31 mM FcMeOH (black line) at a disk Au microelectrode (r_e =2.5 mm) showing discrete current step decreases in the presence of dispersed beads ($r_b = 0.5$ mm, $c_{bead} = 4 \times 10^8$ cm^{-3}) at 0.5 (red line), 5 (blue line), and 50 mM (green line) KCl supporting electrolyte concentrations. (b) Detail of panel a. (c) Ex situ optical micrograph taken after the amperometric measurements showing the electrode surface covered by beads.

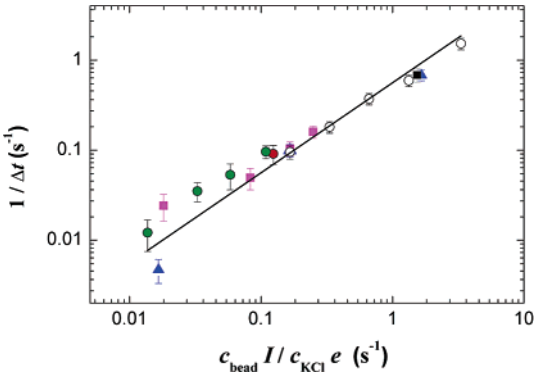

Figure 2. Experimental values for the bead arrival rate plotted vs the grouped variable $c_{bead}I/c_{KCl}$ (log−log scale). Each point is from a separate measurement. Individual variables were varied systematically. (blue triangles) $c_{KCl} = 0.5$, 5 and 50 mM ($I = 0.2$ nA, $c_{bead} = 4 \times 10^8$ cm^{-3}), (red circle) $I = 0.2$ nA, $c_{bead} = 3.2 \times 10^9$ cm^{-3}, $c_{KCl} = 50$ mM, (magenta squares) $I = 0.02$, 0.1, 0.2, and 0.3 nA ($c_{bead} = 4 \times 10^8$ cm^{-3} $c_{KCl} = 5$ mM), (black square) $I = 1.89$ nA, $c_{bead} = 0.4 \times 10^9$ cm^{-3}, $c_{KCl} = 5$ mM, (open circles) $c_{bead} = 0.4$, 0.8, 1.6, 3.2, and 8×10^9 cm^{-3} ($I = 0.2$ nA, $c_{KCl} = 5$ mM), (green circles) $I = 0.06$, 0.16, 0.22, and 0.53 nA ($c_{bead} = 1 \times 10^8$ cm^{-3} $c_{KCl} = 5$ mM). Error bars were evaluated from counting statistics. The solid line is a fit to eq 1 yielding a value of $u_{bead} = 5.6 \times 10^{-8}$ m^2 V^{-1} s^{-1}, in good agreement with values cited in the literature.[5b,c]

($J_{diff} = 4 r_e c_{bead} D_{bead} = 0.002$ s^{-1}, where $D_{bead} \approx 4.4 \times 10^{-9}$ cm^2 s^{-1} is the diffusion coefficient for the conditions used in Figure 1).

As the anodic current controls the bead arrival rate, variation of the applied electrode potential (at constant current within the FcMeOH diffusion-limited region) does not influence bead transport. Steps were not observed when the sign of the current was inverted, i.e., when 1.5 mM ferrocenium methanol was reduced at the electrode surface. In this case, the beads migrate toward the counter electrode, not the Au disk electrode. Previously electrode-

10.1021/ja0478577 CCC: $27.50

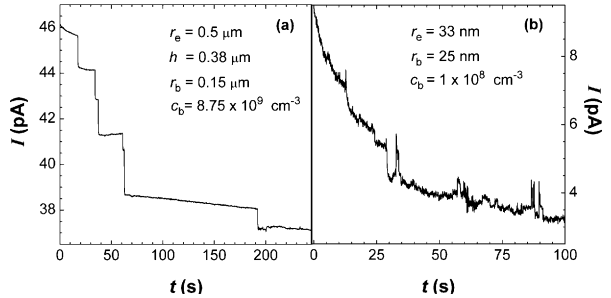

Figure 3. $I-t$ transients showing discrete step decreases in current in the presence of dispersed beads at (a) a lithographically fabricated, recessed Au electrode (c_{KCl} = 5 mM, c_{FcMeOH} = 0.34 mM) and (b) an Au nanoelectrode electrodeposited on an etched Pt wire nanoelectrode insulated with polymer (r_e = 33 nm) in the presence of carboxylate-functionalized core−shell particles (c_{KCl} = 1 mM, c_{FcMeOH} = 0.57 mM).

posited beads were also not removed when the sign of the current was inverted, indicating short-range attractive forces between the electrode surface and the beads for our experimental conditions.

In the measurements described above, the relative size of the current steps, $\langle\Delta I\rangle/I$, where $\langle\Delta I\rangle$ is the average step size,[6] was invariant with c_{salt}, c_{bead}, and I for submonolayer coverage. It is expected that $\langle\Delta I\rangle/I$ should scale with the ratio of electrode to bead radii. To probe this, the above measurements were repeated for a range of electrode radii (individually addressable, lithographically fabricated, recessed disk electrodes with radius r_e = 0.5−5 μm, recessed by h = 0.26−0.38 μm) for r_b = 0.5 and 0.15 μm. $\langle\Delta I\rangle/I$ increased linearly with increasing r_b/r_e (Supporting Information). An example of an $I-t$ transient showing steps corresponding to the detection of 0.15 μm spheres at a 0.5 μm electrode is given in Figure 3a. Furthermore, the detection of 25 nm spheres (carboxylated CdSe Q-particles, Quantum Dot Corp) at a nanometer Au electrode demonstrates that the technique can be scaled down further to the sub-100 nm scale (Figure 3b).

Ex situ images confirm that the beads form closed-packed structures on the electrode surface with a high degree of specificity (Figure 1c). Deposition is not due to sedimentation, as it is independent of sample orientation, and the dependence of J_{mig} on salt concentration is contrary to DLVO theory for particle stability.[7a] It has been previously noted that colloidal particles can assemble at an electrode due to dc electrophoretic deposition,[7b−d] the attractive interaction between beads being effected by the surrounding electroosmotic flows.[8] The effect of Brownian motion is, however, expected to become increasingly relevant as sphere size decreases to the submicron scale.[8b] For nm-scale spheres, the competition between electroosmosis and Brownian motion was experimentally visualized as step oscillations between plateau regions in the $I-t$ response for both the 150 (Figure 4) and 25 nm spheres (Figure 3b). Deposited beads can also rearrange on the electrode surface, giving rise to extra steps or abrupt *increases* in the current.

Simulation of the diffusion problem for our electrode−bead system shows that ∼50% of the current decrease occurs as the bead moves from a distance ∼5r_b to a distance ∼r_b from the surface (Supporting Information). This makes the technique independent of the adsorption mechanism at the electrode, greatly broadening its applicability. For complete monolayer coverage, the calculated total drop in current is 35% (Supporting Information). This value is consistent with experimental observations at low current, low c_{bead}, and high c_{KCl}. For other conditions, a larger decrease in the

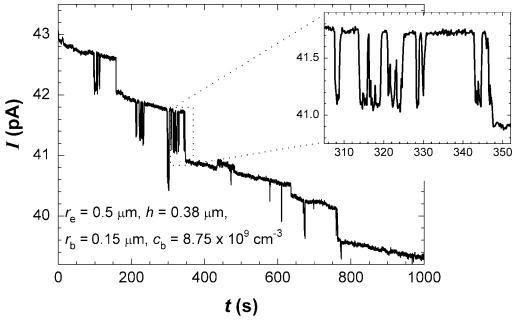

Figure 4. $I-t$ response for a fabricated electrode showing both current oscillations and abrupt increases (c_{KCl} = 5 mM, c_{FcMeOH} = 0.5 mM). The inset is a magnification of a region where rapid oscillations in current were observed.

current was observed, indicating that multilayers of beads are formed (e.g., red line in Figure 1a).[7d] The step size is predicted to decrease with increasing surface coverage, as the beads' relative influence on FcMeOH mass transfer is less. Experimentally, this was seen as a gradual smearing out of ΔI at long times until it could no longer be resolved above the background noise.

The detection technique described here can in principle be scaled down to detect individual molecules preferentially binding at nanometer electrodes. In this case, the flux of particles would be primarily due to diffusion rather than electrophoresis. For example, a protein (e.g., glucose oxidase, Gox, $r_b \approx 5$ nm) binding at a $r_e \approx$ 15 nm electrode would yield a diffusive rate $1/\Delta t \approx J_{diff} = 0.08$ s^{-1} ($D_{GOx} = 4.3 \times 10^{-7}$ cm^2 s^{-1}, $c_{GOx} = 50$ pM), much larger than the corresponding electrophoretic rate given by eq 1, $J_{mig} = 1.3 \times 10^{-4}$ s^{-1} (I = 30 pA, c_{salt} = 50 mM, $u_{GOx} = 3.4 \times 10^{-10}$ m^2 s^{-1} V^{-1}).[9] From $r_b/r_e = 0.33$ we predict a $\langle\Delta I\rangle/I_0$ value of ca. 2%, a readily measurable signal.

Acknowledgment. This research was funded by Stichting voor Fundamenteel Onderzoek der Materie (FOM) and The Netherlands Organization for Scientific Research (NWO).

Supporting Information Available: Additional experimental details and simulations. This material is available free of charge via the Internet at http://pubs.acs.org.

References

(1) (a) Gu, L.-Q.; Cheley, S.; Bayley, H. *Science* **2001**, *291*, 636−640. (b) Sun, X.; Jin, W. *Anal. Chem.* **2003**, *75*, 6050−6055. (c) Gilardi, G.; Fantuzzi, A. *Trends Biotechnol.* **2001**, *19*, 468−476.
(2) Gorschlüter, A.; Sundermeier, C.; Ross, B.; Knoll, M. *Sens. Actuators B* **2002**, *85*, 158−165.
(3) All measurements used a potentiostat (BAS CV-50W) in a three-electrode arrangement with the Au microelectrode, an Ag/AgCl electrode (BAS), and a Pt wire as working, reference, and counter electrodes, respectively.
(4) Bard, A. J.; Faulkner, L. R. *Electrochemical Methods, Fundamentals and Applications*, 2nd ed.; John Wiley & Sons: New York, 2001.
(5) (a) $u_{K+} \approx u_{Cl-} \approx 7.79 \times 10^{-8}$ m^2 V^{-1} s^{-1}, $u_{bead} \approx 4.5$, 5.5, and 3×10^{-8} m^2 V^{-1} s^{-1} at 0.5, 5, and 50 mM KCl, respectively.[5b,c] (b) El-Gholabzouri, O.; Cabrerizo-Vílchez, M. A.; Hidalgo-Álvarez, R. *J. Coll. Int. Sci.* **2003**, *261*, 386−392. (c) Vorweg, L.; Antonietti, M., Tauer, K. *Colloids Surf. A* **1999**, *150*, 129−135.
(6) As ΔI for each event depends on the site of bead approach to the disk electrode (edge vs center), we report the average $\langle\Delta I\rangle$.
(7) (a) Kun, R.; Fendler, J. H. *J. Phys. Chem. B* **2004**, *108*, 3462−3468 and references therein (b) Trau, M.; Saville, D. A.; Aksay, I. A. *Science* **1996**, *272*, 706−709. (c) Böhmer, M. *Langmuir* **1996**, *12*, 5747−5750. (d) Gersig, M.; Mulvaney, P. *J. Phys. Chem.* **1993**, *97*, 6334−6336.
(8) (a) Solomentsev, Y.; Böhmer, M.; Anderson, J. L. *Langmuir* **1997**, *13*, 6058−6068. (b) Solomentsev, Y.; Guelcher, S. A.; Bevan, M.; Anderson, J. L. *Langmuir* **2000**, *16*, 9208−9216.
(9) Matsumoto, N.; Chen, X.; Wilson, G. *Anal. Chem.* **2002**, *74*, 362−367.

JA0478577